

Preclinical Justification of pbi-shRNA EWS/FLI1 Lipoplex (LPX) Treatment for Ewing's Sarcoma

Donald D. Rao¹, Christopher Jay¹, Zhaohui Wang¹, Xiuquan Luo¹, Padmasini Kumar², Hilary Eysenbach¹, Maurizio Ghisoli^{3,4,5}, Neil Senzer^{2,3}, John Nemunaitis^{2,3,4,5}

¹Strike Bio, Carrollton, Texas, USA; ²Gradalis, Inc., Dallas, Texas, USA; ³Mary Crowley Cancer Research Centers, Dallas, Texas, USA; ⁴Texas Oncology, P.A., Dallas, Texas, USA; ⁵Medical City Dallas Hospital, Dallas, Texas, USA

The EWS/FLI1 fusion gene is well characterized as a driver of Ewing's sarcoma. Bi-shRNA EWS/FLI1 is a functional plasmid DNA construct that transcribes both siRNA and miRNA-like effectors each of which targets the identical type 1 translocation junction region of the EWS/FLI1 transcribed mRNA sequence. Previous preclinical and clinical studies confirm the safety of this RNA interference platform technology and consistently demonstrate designated mRNA and protein target knockdown at greater than 90% efficiency. We initiated development of pbi-shRNA EWS/FLI1 lipoplex (LPX) for the treatment of type 1 Ewing's sarcoma. Clinical-grade plasmid was manufactured and both sequence and activity verified. Target protein and RNA knockdown of 85–92% was demonstrated *in vitro* in type 1 human Ewing's sarcoma tumor cell lines with the optimal bi-shRNA EWS/FLI1 plasmid. This functional plasmid was placed in a clinically tested, liposomal (LP) delivery vehicle followed by *in vivo* verification of activity. Type 1 Ewing's sarcoma xenograft modeling confirmed dose related safety and tumor response to pbi-shRNA EWS/FLI1 LPX. Toxicology studies in mini-pigs with doses comparable to the demonstrated *in vivo* efficacy dose resulted in transient fever, occasional limited hypertension at low- and high-dose assessment and transient liver enzyme elevation at high dose. These results provide the justification to initiate clinical testing.

Received 29 February 2016; accepted 22 April 2016; advance online publication 19 July 2016. doi:10.1038/mt.2016.93

INTRODUCTION

Ewing's sarcoma is the second most frequently diagnosed primary malignant bone tumor in children in the United States¹ with an annual incidence of 2.9 cases per million population.² Up to 85% of Ewing's tumors are characterized by the EWS/FLI1 (11;22) (q24;q12) translocation designated as the EWS/FLI1 fusion gene.³ Types I and II fusions comprise 60 and 25%, respectively, of the documented breakpoint sites.⁴

The EWS/FLI1 fusion gene plays a key role in Ewing's sarcoma pathogenesis and maintenance and is universally designated as the dominant driver gene.^{5–7} Ewing's sarcoma fusion gene breakpoint

sites are optimal targets for sarcoma specific RNA interference (RNAi)-mediated knockdown^{8,9} that has demonstrated preclinical therapeutic efficacy in both *in vitro* and *in vivo* testing. In a variety of models, both antisense oligonucleotides^{10,11} and siRNAs^{12–20} have confirmed targeting relevance and have proven safe in conjunction with down regulation of EWS/FLI1 gene expression.

Sixty to eighty percent of Ewing's sarcoma patients present with primary metastatic disease and will experience relapse or refractory progression.^{1,21–24} The median time to relapse is 1.3 years and those who relapse have a poor 1-year/5-year survival from time of relapse.^{1,21} Few respond to second-line therapy and fewer achieve a second remission. Consequently, 5-year survival is severely limited,^{1,21,25–29} particularly so in patients with “high-risk” disease (*i.e.*, those with relapse within 2 years of front line treatment). In one large retrospective analysis of 714 patients from time of first relapse, the 1-year overall survival (OS) was 43%, 5-year OS was 13%, and 10 year OS was 9%.²¹ However for patients with relapses that occurred within the first 2 years after initial diagnosis, the 2-year OS was 7%²⁶ and the 5-year event free-survival was 5%.²⁹

Second-line chemotherapy for relapsed Ewing's sarcoma has likewise shown limited efficacy with only 9 to 13% of patients achieving a second disease-free remission.^{27,29,30} There is no standard of care for second-line treatment. Regimens such as topotecan/cyclophosphamide, irinotecan/temozolomide, or docetaxel/gemcitabine have been utilized in second line or later treatment and may prolong life for those who respond.^{31–44}

Unfortunately, for the majority of relapsed patients who do not respond to second-line chemotherapy or who relapse following a second remission, the prognosis is grim with no significant benefit of third-line chemotherapy.^{27,30} In a relatively large retrospective analysis of 195 patients, of the 86% whom did not achieve second remission 97% had died with a median survival of 11.7 months and no patient achieved disease control. Of the 26 patients who achieved a second remission, 12 relapsed and none experienced a third remission (10/12 died and in the first year and 2 were living with uncontrolled disease at 6 and 13 months).²⁹ Thus, there is desperate need for the development of newer, more effective treatment options in the metastatic, “high risk”, and post-relapse Ewing's population.

RNAi is a natural cellular regulatory process capable of inhibiting transcriptional, post-transcriptional and translational

mechanisms thereby modulating gene expression. Using a miR30-scaffold, we developed a novel "bifunctional" RNAi strategy, which demonstrated effective silencing of target gene expression by concurrently inducing post-transcriptional RNA-induced silencing complex (RISC) cleavage-dependent mRNA cleavage and RISC cleavage-independent translational repression and p-body sequestration.⁴⁵

We have expanded these observations and have demonstrated significant reduction of *EWS/FLI1* gene expression using a novel bi-shRNAi platform and delivery LPX (lipoplex) that resulted in inhibition of Ewing's tumor growth *in vitro* and safety as well as a survival advantage *in vivo*.

RESULTS

Target site justification

We identified specific *EWS/FLI1* fusion breakpoints and engaged lateral sequence single-step assessment for optimization of the bifunctional shRNA (bi-shRNA) target sequence across the fusion region. The bi-shRNA is specific to *EWS/FLI1* type 1 fusion gene. We designed three bi-shRNAs encompassing the fusion mRNA joint region with slightly divergent sequences; plasmids pGBI 140, 141, and 142 (Figure 1b). The expression units for the bi-shRNAs targeted to the type 1 *EWS/FLI1* fusion breakpoint was assembled and inserted between the Sal I and Not I sites of mammalian expression vector pUMVC3 from which the shRNA expression is driven by an enhanced pol II CMV promoter (Figure 1a).⁴⁶ The final bi-shRNA *EWS/FLI1* construct contains two stem-loop structures in a previously described modified miR-30a backbone⁴⁷ One of the stem-loops consists of fully matched passenger and guide strands (RISC cleavage-dependent; the siRNA component), whereas the other stem-loop structure contains four base-pair mismatches between passenger and guide strands (RISC cleavage-independent; the miRNA-like component). The nucleotide mismatches in the latter are at positions 9 to 11 and 17 of the passenger strand, which create a mismatch at the central location and seed region similar to most miRNAs.⁴⁸ By placing the mismatches in the passenger strand, the siRNA and miRNA-like guide strands are complementary to the identical mRNA target sequence strand thereby further limiting the potential for off-target side effects. The predicted stem-loop structure of plasmid pGBI 140 is graphically shown on Figure 1c. The targeting sequence was carefully analyzed for potential cross-reactivity to other human mRNAs by BLAST search. The optimum targeting sequence based on our proprietary algorithm with the least off-target side effects, was used to design the expression vector constructs. The Ewing's type 1 construct target sequence and the schematic of the expression plasmid is shown in Figure 1a, b, respectively. The final construct was sequence confirmed in its entirety and then reconfirmed three times as part of GMP DNA and lipoplex manufacturing process.

In vitro activity of bi-shRNA *EWS/FLI1* plasmid

Target gene expression knockdown was first tested *in vitro*. The three constructs of the pbi-shRNA *EWS/FLI1* plasmid, vectors pGBI 140, 141 and 142 (spanning the Ewing's type 1 junction region), were tested. SK-N-MC human Ewing's sarcoma cells have the Ewing's type 1 translocation and the type 1 fusion gene expression at the mRNA level was further confirmed using

reverse transcription polymerase chain reaction (RT-PCR) (data not shown). The functional outcome of knockdown was demonstrated by selective growth inhibition of the SK-N-MC cells *in vitro* (Figure 2b). The growth of HEK-293 cells, control cells not containing the *EWS/FLI1* fusion, to assess effect on normal, nontranslocated *EWS* and *FLI1* genes, was not affected even with a 10-fold higher concentration of bi-shRNA *EWS/FLI1* DNA exposure. The transfection efficiency for HEK-293 cells and for SK-N-MC cells was monitored by reporter gene and both cell lines were over 80% efficiency. Initial *in vitro* testing of three bi-shRNA constructs traversing the targeting type I fusion region (targeting sequence is shown on Figure 1b) revealed 85–92% knockdown of the fusion gene assayed by FLI1 (Figure 2a) antibody. Although the empty vector (pUMVC3) also affected the expression of fusion protein, the bi-shRNA expressing vector showed the optimal effect. Depending on the gene target and the transfection condition used, we often observe a lower level of target gene expression reduction with the empty vector control possibly due to recovery from the transfection condition. Comparative sequence analysis of the fusion region from *EWSR1* and *FLI1* demonstrated that the sequence is completely conserved between human, mouse, rat, and pig. Therefore, rodents and pigs are bio-relevant models for efficacy and toxicology analysis of the pbi-shRNA *EWS/FLI1* LPX.

In vivo murine efficacy and safety of pbi-shRNA *EWS/FLI1* LPX

For *in vivo* studies, the payload plasmid DNA was complexed with the cationic liposome for systemic delivery. The cationic liposome and DNA complex (lipoplex) have been utilized in numerous *in vivo* and clinical studies.⁴⁹ Lipoplex formulation has been optimized for bi-shRNA *EWS/FLI1* vectors. A series of three independent efficacy studies were carried out. The pbi-shRNA *EWS/FLI1* LPX demonstrated a reduction in tumor growth and improved survival in a dose-responsive manner in all three independent SK-N-MC Ewing's sarcoma subcutaneous implanted xenograft mouse model studies without adverse or toxic effect. Study mice gained weight throughout the study period; however, no significant differences in body weight were observed between control and treated mice or between low-dose and high-dose cohorts. Survival benefit supported the efficacy of the pbi-shRNA *EWS/FLI1* LPX. A statistically significant dose-related tumor growth inhibition was seen in two independent xenograft studies (Studies # e203 and 207, Figure 3a, c). Moreover, a statistically significant dose-related survival advantage was demonstrated in a third xenograft trial (Study # e204, Figure 3b). Notably 100% of high-dose pbi-shRNA *EWS/FLI1* LPX-treated xenograft mice were alive at day 28 after dosing initiation compared to less than 20% survival in control mice (study animals were terminated when tumor exceeded the maximum allowed tumor volume). As noted, the tumor response and animal survival benefit was highly significant ($P \leq 0.001$) in all studies.

As part of the process of optimization of the manufacture of the pbi-shRNA *EWS/FLI1* LPX to improve scale-up opportunity, we reduced product particle size by two- to threefold and minimized variability of size in compliance with FDA recommendations for clinical application. The previous manufacturing technique utilized a thin-film method. The average of 10 independent DNA-Lipoplex batches resulted in a mean particle size

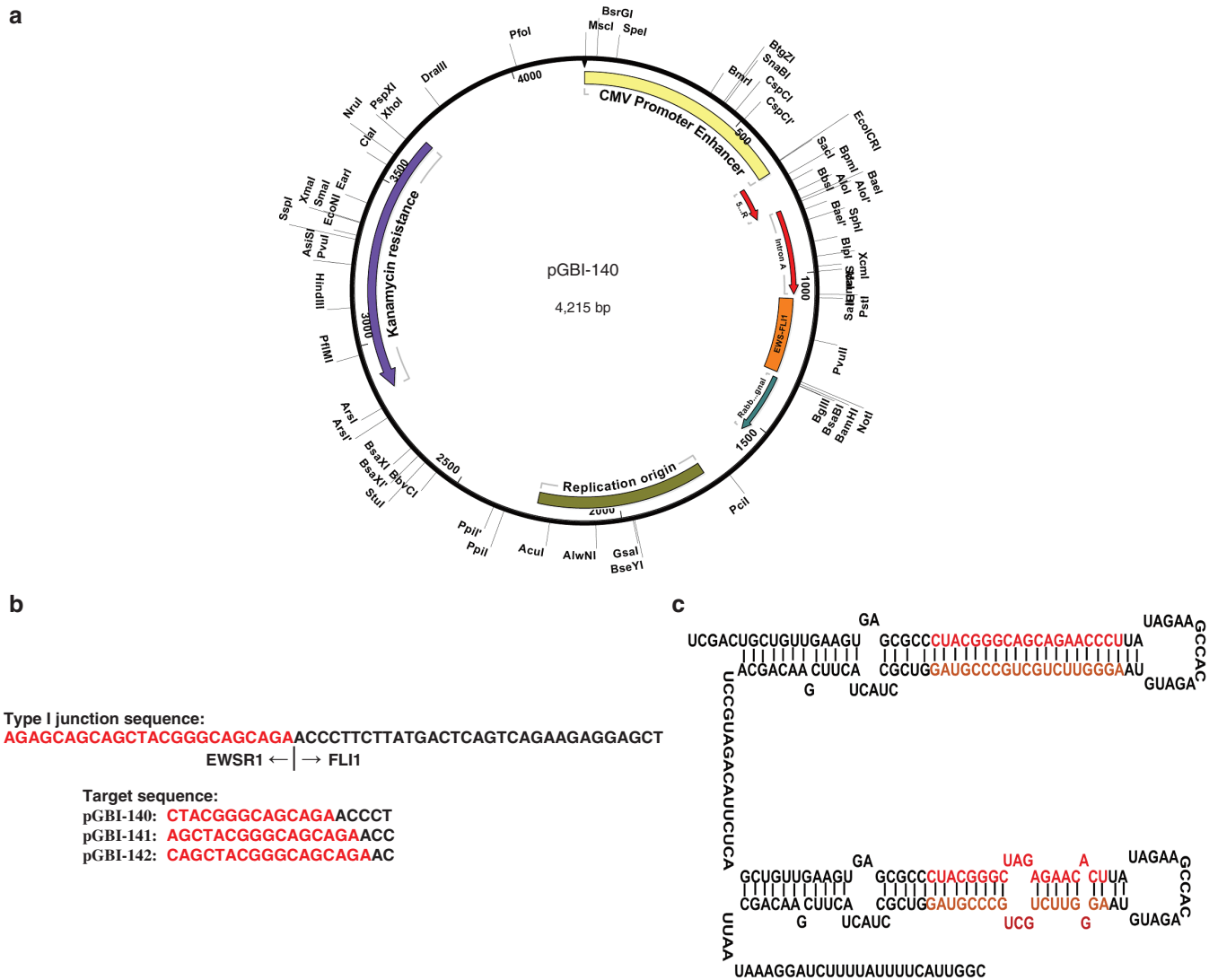


Figure 1 bi-shRNA^{EWS-FLI1} construct and target sequence. **(a)** Circular diagram of bi-shRNA^{EWS-FLI1} construct (pGBI-140). Key vector elements and single cut restriction sites are shown. **(b)** Target sequence for pGBI-140, -141, and -142 in relation to the translocation break point sequence. **(c)** Predicted secondary structure of the primary transcript of bi-shRNA^{EWS-FLI1} (pGBI-140). The predicted stem-loop structure is first processed in the nucleus by the microprocessor complex before transported into the cytoplasm.

of 426 ± 56 nm with a mean polydispersity index of 0.592 ± 0.115 . The optimized manufacturing process utilizes a rapid injection liposome technique. The mean particle size of four independent DNA-Lipoplex was 169 ± 16 nm with a mean polydispersity index of 0.226 ± 0.025 . The third xenograft efficacy study (Study # e207) utilized this optimized manufacturing process (Figure 3c). Target gene (measured by FLI-1 antibody) and downstream fusion protein induced gene (CD99) knockdown *in vivo* was demonstrated by western immunoblot on xenografted tumor tissues after four rounds of treatment with various doses (Study # e208, Figure 4). The fusion gene protein expression knockdown ranged from 64 to 84% (Figure 4, lanes 3–6) with reduction in CD99 protein expression from 21 to 72%. CD99 is a well-known Ewing's induced cell surface protein often used to differentiate Ewing's sarcoma from other sarcomas.^{50–52} The western assay on *in vivo* tumor samples was done with small tumor sections sampled from different regions of the whole tumor; although the knockdown percentage

varies site to site (a representative results is shown on Figure 4), reduction of target fusion gene expression and induced CD99 expression was consistent. Results shown in Figure 5 display the cytokine response to a single high dose of pbi-shRNA EWS/FLI1 (100 µg IV) in Balb/c mice.

Cytokine response

Results are consistent with toxicity response highlighted by transient fever in mini-pigs shown below. Rapid induction of IL6, IL12, and TNF following dosing is observed with return to baseline within 10 hours. Circulating IFNγ was also observed in male mice over the same time course.

Toxicology dose range study of bi-shRNA EWS/FLI1 LPX in pigs

A dose range toxicology study was performed in mini-pigs (Charles River Laboratories, Spencerville, OH) to determine the maximum

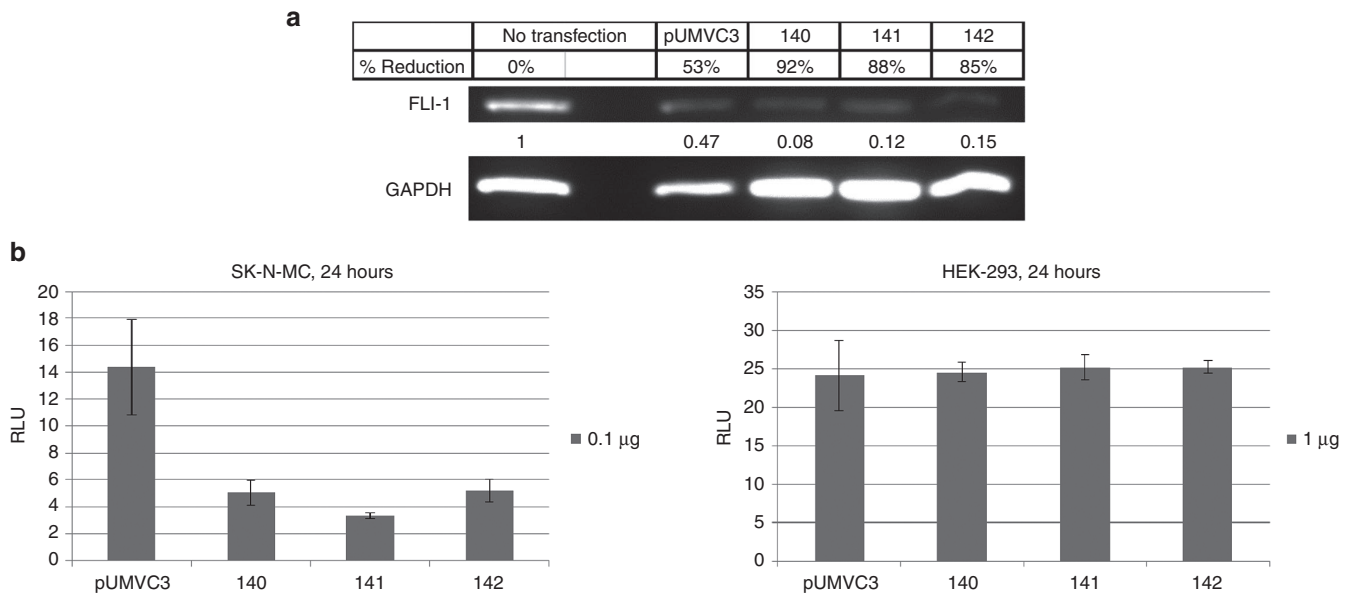


Figure 2 Target gene expression knockdown and EWS-FLI1 selective growth inhibition of Ewing's sarcoma cells (SK-N-MC, type I mutation). **(a)** SK-N-MC cells were transfected with 0.1 µg of each plasmid DNA by electroporation. Two days after transfection, cells were lysed with CellLytic MT solution and process for western immunoblot. The Ewing's type 1 fusion protein was detected via antibody to FLI-1 and percentage reduction in expression was obtained by normalizing fusion protein expression to GAPDH expression. **(b)** SK-N-MC cells or HEK-293 cells (embryonic kidney cell line without EWS-FLI1 fusion) were transfected with 0.1 or 1 µg of plasmid DNA by electroporation, respectively. After electroporation, cells were plated in 96-well and assayed for growth with CellTiter-Glo Luminescent Cell Viability Assay measuring relative light units (rlu) at 24 hours after. No effect was observed on cells not containing EWS/FLI1 fusion. pUMVC3 is the empty vector control; 140, 141, and 142 are different fusion region targeting constructs.

tolerated dose (MTD) with biweekly intravenous infusions for 4 weeks of the pbi-shRNA EWS/FLI1 LPX utilizing the optimized manufacturing process. Two dose levels were tested, 0.128 mg/kg (low) and 0.384 mg/kg (high), equivalent to 25 and 75 µg infusion per mouse, respectively. The predicted human equivalents of these dose levels are 0.0846 and 0.2538 mg/kg, respectively.

pbi-shRNA EWS/FLI1 LPX-related increases in body temperature were noted 2 to 4 hours following dosing on Days 1 and 5 in both high- and low-dose cohorts. The elevated body temperatures coincided with transient shivering, decreased activity, and vomiting. An additional dose of Meloxicam (equivalent to acetaminophen use in patients) was administered for temperature above 104°F (40 °C) within 6 hours after post-dose response. By 24 hours, the body temperatures returned to normal in all pigs. On Day 5, two high-dose female animals with temperatures above 102°F were administered an additional dose of Meloxicam. None required Meloxicam intervention after the second treatment.

There were no pbi-shRNA EWS/FLI1 LPX-induced changes in body weight, coagulation parameters, gross pathology, or organ weights. Transient pbi-shRNA EWS/FLI1 LPX-related decreases up to 80% in the total white blood cell count and neutrophils were noted in ≥ 0.128 mg/kg-treated animals compared to the controls beginning either 6 or 24 hours post-each dose administration and continuing through 48 hours. No dose-related adverse effect on renal function was seen based on the serum creatinine and blood urea nitrogen levels throughout the course of the treatment.

One 0.384 mg/kg male (study animal #7326) displayed decreased activity with tremors, head tilt, and coughing, and was euthanized on Study Day 21. A thrombus was noted in the right jugular vein at necropsy. This was confirmed microscopically and

attributed to the presence of the venous access port. Microscopic observations of multifocal mild bronchioloalveolar mixed cell infiltrates and minimal intra-alveolar fibrin suggest a compromise of capillary/alveolar membranes. The justification to sacrifice this pig was considered related to complications from the vascular access port.

Serological evidence of liver irritation was demonstrated in a subset of the high-dose pigs. Pig #7326, who was terminated early, had slight rise in bilirubin to 2.85 mg/dl with return to normal on day 3 (0.19 mg/dl); no other significant bilirubin rises were noted in other pigs. Transient alkaline phosphatase rise was noted in all high-dose pigs and transient increases in GGT levels rarely above 200 U/l was seen in pigs 7326 and 7328. No microscopic liver pathology was observed at final sacrifice (3 days after last dose). No low-dose pigs showed liver irritation (see **Figure 6**). The blood alkaline phosphatase level was elevated two to threefold for 2 days post-treatment after each dosing in the 0.384 mg/kg group. It was only slightly elevated in the 0.128 mg/kg group. Animal #7327 of the 0.384 mg/kg group had normal alkaline phosphatase level after four doses. Blood AST level transiently elevated eight to ninefold for #7326 two days after treatment, but was only slightly elevated with subsequent treatment. On the other hand, #7328's (female, 0.384 mg/kg cohort) had AST elevation amplified as more doses were given. It is not clear why control animal #7319 also had a significant aspartate aminotransferase (AST) spike on the day 22 dose. #7328 (high dose) had slight increase following the second and third dose. The 0.128 mg/kg cohort had only a slight increase of blood total bilirubin (TBIL) level on the first day of the first dose, the TBIL level returned to normal with subsequent doses. Blood GGT level was not elevated for 0.128 mg/kg group, but did

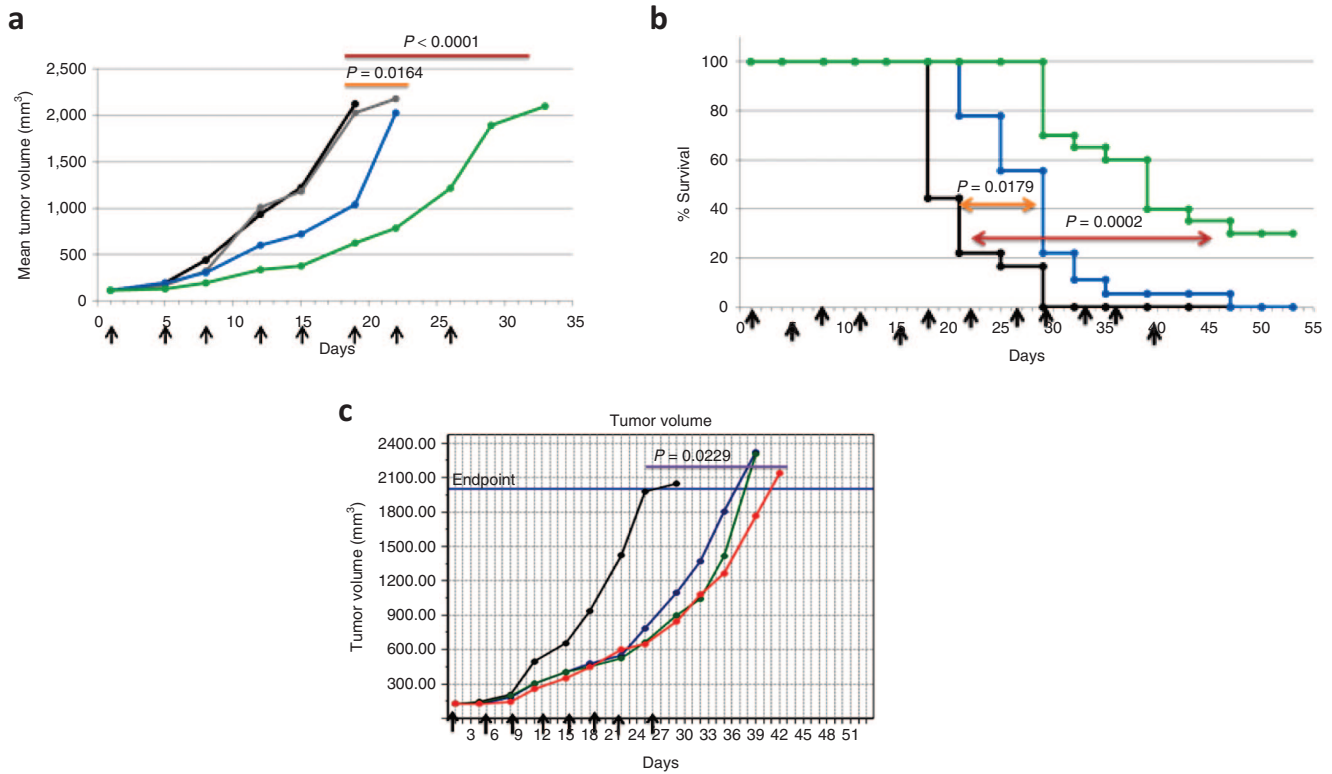


Figure 3 Tumor growth inhibition characterized with SK-N-MC xenograft model. **(a)** Study # e203- Tumor volume change demonstrating marked dose related tumor growth control with both higher dose (25 µg, green line) and lower dose (5 µg, blue line) of two bi-shRNA^{EWS/FLI1} LPX constructs when compared to no treatment (black line) and vehicle control (gray line). Treatment was twice weekly for four weeks. Graph is average of 10 animals per group. **(b)** Study # e204- Dose–response experiment assessing percent of animals alive (tumor did not reach the maximum allowed tumor size) with slightly elevated doses and extended treatment time to 6 weeks. Kaplan-Meier survival curve showed survival advantage with high dose groups (25.0 and 18.75 µg dose groups, green line) compared with low-dose groups (12.5 and 6.25 µg dose groups, blue line) and no treatment and vehicle control group (black line). Ten animals were assessed per group. **(c)** Study # e207- Tumor growth inhibition of bi-shRNA^{EWS/FLI1} LPX (using improved LP) assessed with further escalated doses; 25 µg (blue line), 50 µg (green line), 75 µg (red line) and control (black line). Treatment was twice weekly for four weeks and tumor measurements over 45 days post the initiation of the treatment. Graph shown is the medium of 10 animals per group. Arrows indicate IV infusion time points.

rise three to fivefold in #7326 (high dose) throughout the course of the treatment (Figure 6), it might be worth noting that #7326 already had slightly higher GGT level 6 days prior to treatment. #7328's GGT elevated following the second dose (which was not typically observed ≥ second dose) and the GGT level was significantly higher throughout. Sporadic low level increases in lactate dehydrogenase (LDH) and creatine kinase (CK) were also noted at 0.128 and 0.384 mg/kg at 6 to 24 hours following dosing.

Transient drops in systolic blood pressure to below 90 were considered significant. This was observed in one low-dose pig (#7323) intermittently throughout the course of treatments but not related to time of administration. However, pretreatment transient drops in systolic blood pressure were also observed to a similar degree. This pig also had frequent no readings from the vascular monitoring probe, thereby suggesting sensor probe function variability. The blood pressure readings were not correlated to clinical sequelae. One other pig (#7322, low dose) had a systolic blood pressure of 86 on Day 8 of testing also without other clinical sequelae. These were considered insignificant. No compromise or cardiac work load was observed.

Microscopic findings were observed and included mild to marked thrombosis at the primary administration site (vascular access port)

and the presence of numerous granulocytic and mononuclear cells within affected alveoli and bronchioles in the lungs. Thrombosis was evident in variably-sized pulmonary vessels. The pulmonary thrombi were interpreted as a secondary event following embolization from the primary administration site and a possible source for compromise of the capillary wall/alveolar epithelial barrier and local pulmonary circulation. Minimal to moderate interstitial accumulations of mononuclear cells adjacent to airways and vessels were considered secondary to changes occurring within the alveoli. The findings noted in the lung were not considered direct test article effects.

DISCUSSION

In vitro results confirmed the efficacy of pbi-shRNA EWS/FLI1 LPX with marked knockdown of Ewing's type 1 fusion protein correlating with tumor growth reduction. Moreover, specificity was observed with no evidence of tumor growth reduction in tumor cells not containing the EWS/FLI1 fusion gene. Humans, rodents, and pigs have identical sequence matching at the exons involved in the translocation of *EWS* and *FLI1* genes, supporting bio-relevance of these animal models for safety studies. Reasonable tolerance was observed in both mice and pigs to pbi-shRNA EWS/FLI1 LPX with acceptable safety at the low dose level of 0.128 mg/

kg (human equivalent of 0.0846 mg/kg). Moreover tumor growth inhibition in multiple Ewing's type 1 tumor xenograft studies supported efficacy as measured by dose-related tumor response and survival. Demonstration of target gene knockdown in the treated xenografted tumors verified the modality of drug action in correlation with tumor response and survival advantage.

The *EWS/FLI1* translocation results in aberrant expression of a novel fusion transcription factor which affects several signal pathways and cellular phenotypes.^{5,51} We first demonstrated *EWSR/FLI1* knockdown in the type 1-specific SK-N-MC cell lines *in vitro*. SK-N-MC cells are difficult to transfect by standard transfection methods⁵¹; thus, we used electroporation to effect plasmid delivery *in vitro*. The electroporation process has limits with respect to cell viability. As demonstrated by western immunoblot analysis, our constructs did efficiently reduce the expression of *EWSR/FLI1* fusion protein, but the empty vector control (pUMVC3) also resulted in some reduction of *EWSR/FLI1* fusion protein. The housekeeping gene for the load control (Glyceraldehyde 3-phosphate dehydrogenase (GAPDH)) was also lower (when compared with other samples); it appears that there is a generalized reduction in both *EWSR/FLI1* and GAPDH proteins. The probing of GAPDH and *EWSR/FLI1* was on the same blot and was not related to gel loading. The GAPDH protein expression was not affected in bifunctional shRNA construct transfected cells. Further assessment is underway.

To demonstrate pharmacodynamics, we examined *EWSR/FLI1* protein expression in treated tumor compared to untreated tumor or vehicle treated control. As shown on **Figure 4**, tumors obtained from various dose-treated animals were shown to have significant target protein knockdown. SK-N-MC tumor is a well-vascularized tumor,⁵³ thus sections examined by western immunoblot may contain varied numbers of host cells distorting accurate quantification of *EWSR/FLI1* protein, which may limit dose-related knockdown efficiency assessment. We also examined *CD99* expression, which is highly expressed in Ewing's sarcoma cells. Although Chromatin Immunoprecipitation (CHIP) analysis in one study suggests *EWSR/FLI1* fusion protein binds to the promoter region of *CD99*, changes in *CD99* expression have not been consistent across other studies.⁵¹ A recent paper suggests the *EWS/FLI1* RNAi effect on *CD99* expression is effected instead at the post-transcriptional level.⁵⁴ As shown on **Figure 4** bottom panel, *CD99* protein was substantially reduced. Assessment of dose response was limited but results are consistent with target gene knockdown effect and consequent phenotype control regardless of mechanism. *EWSR/FLI1* fusion expression is low, and thus difficult to visualize by immunohistochemistry, which was attempted.

The bi-shRNA platform fulfilled clinical release criteria and demonstrated significant and consistent activity in preclinical and clinical testing in adult and pediatric cancer patients thereby providing further confidence with activity of pbi-shRNA *EWS/FLI1* LPX.⁵⁵⁻⁶¹

Additional safe preclinical and clinical experience has been described with another bi-shRNA plasmid/LPX delivery vehicle targeting Stathmin 1 (*STMN1*),^{55,62} a microtubule modulating protein.⁵⁵ This systemic LPX delivery vehicle which also incorporates 1,2-dioleoyl-3-trimethylammonium-propane (DOTAP) and cholesterol^{63,64} and is similar in composition to the vehicle used for the bi-shRNA *EWS/FLI1* plasmid delivery, demonstrated

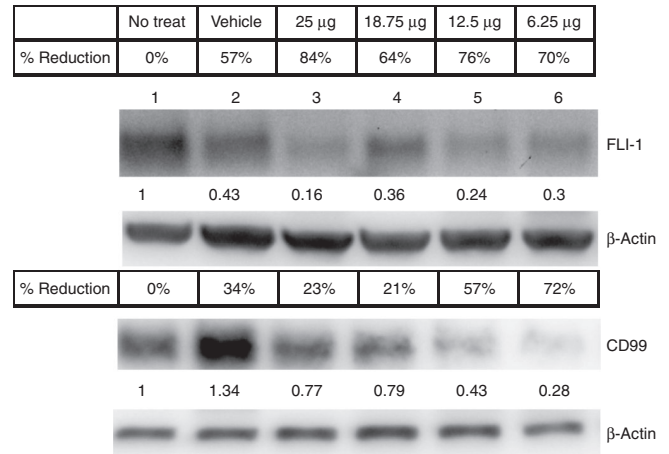


Figure 4 Ewing's fusion protein expression knockdown demonstrated *in vivo*. Study # e205-Nude mice carrying SK-N-MC xenograft were treated with 25 µg (lane 3), 18.75 µg (lane 4), 12.5 µg (lane 5), and 6.25 µg (lane 6) of bi-shRNA^{EWS/FLI1} LPX through slow tail vein infusion at three animal per treatment. The treatment started when tumor was 100–150 mm³ in size, the treatment was twice weekly for 2 weeks. Two days after the final treatment, tumors were taken out and half of the tumors were immersed in Allprotect tissue reagent (Qiagen, Valencia, CA) for molecular analysis. Sections of tumor in Allprotect tissue reagent were processed for western immunoblot with antibody for FLI-1 and for CD99. The fusion protein and CD99 expressions were normalized against β-Actin for comparison. Tumors from untreated (lane 1) and vehicle treated (lane 2) animals were used for comparison. This figure shows a representative result of tumor tissue slices and tumors examined.

the predicted stathmin cleavage product via next-generation sequencing as well as by RNA ligase-mediated rapid amplification of cDNA Ends (RLM-RACE) testing of tumor samples from treated patients.⁵⁵

The delivery vehicle used for bi-shRNAi *STMN1* vector delivery as well as other plasmid based products by us^{65,66} and others^{49,59,67,68} has recently been modified to more explicitly conform to GMP production operation and product release criteria under FDA oversight. This newly modified delivery vehicle was used for the bi-shRNA *EWS/FLI1* delivery. The manufactured liposome/DNA Lipoplex (LPX) are uniquely flexible⁶³ and effectively penetrate functional and physical barriers including passage against interstitial pressure gradients and into tumors across tight endothelial cell barriers.^{64,69} The fusogenic nature of LP allows bypassing of endocytosis mediated DNA cell entry, which could otherwise lead to nucleic acid degradation and contribute to toll-like receptor-mediated off-target effects. Early proinflammatory response induced by siRNA with nonviral liposome delivery systems previously^{70,71} showed induced IL-6 levels as high as 500–600 pg/ml 6 hour post-treatment with 50 µg per mouse infusions whereas our data showed our formulation to have a reduced IL-6 induction of 60–170 pg/ml 6 hours post-treatment with double the infusion dose (100 µg) per mouse; the magnitude of cytokine response thus appears significantly lower than observed by others. This may be part of the reason this formulation is better tolerated in mice, even at higher doses, than other reported lipoplex formulations. These other formulations reach MTD between 35 to 50 µg per 20g mouse, a human equivalent dose of 0.118 to 0.169 mg/kg. In our study similar sized mice tolerated

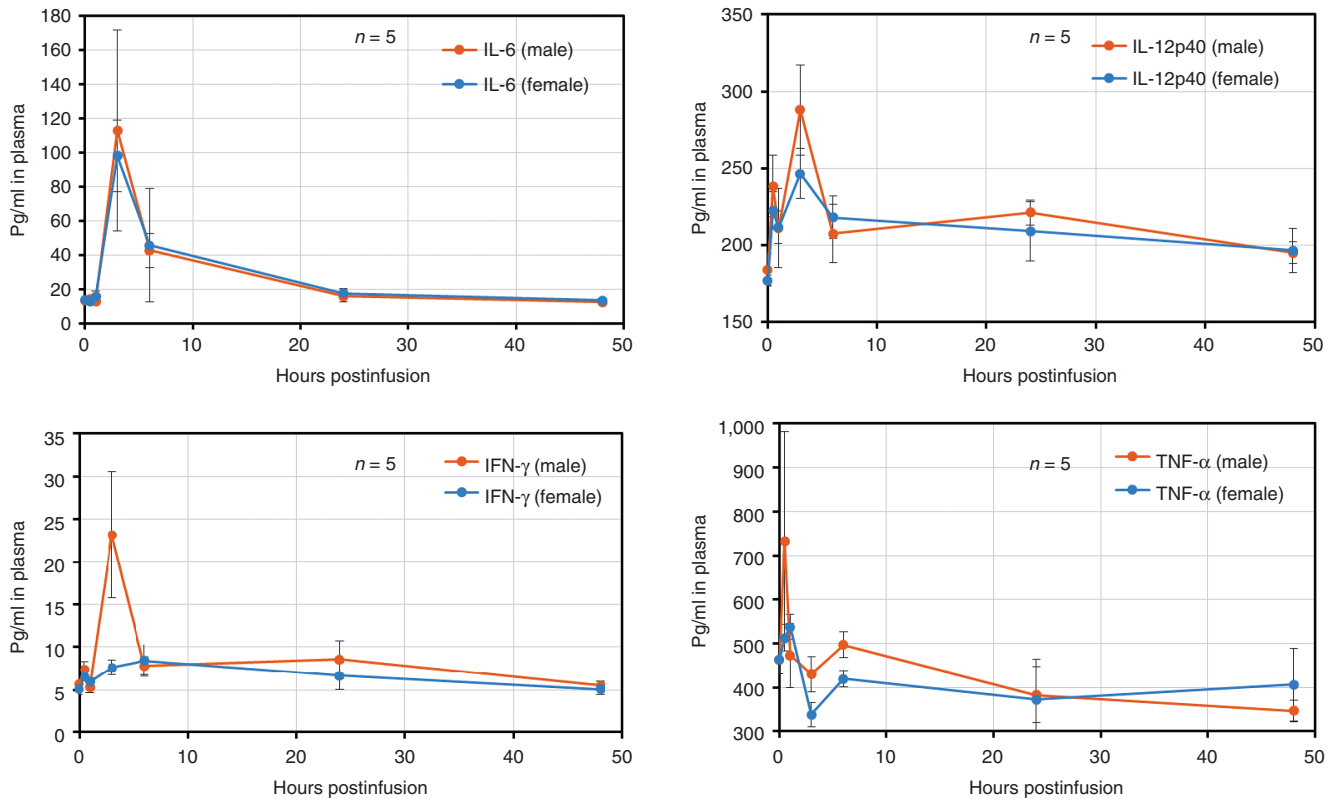


Figure 5 Induction of proinflammatory cytokines by bi-shRNA^{EWS/FLI1} LPX. Five male and five female Balb/C mice were administrated with single dose of 100 μ g bi-shRNA^{EWS/FLI1} LPX via slow tail vein infusion. At 1, 3, 6, 24, and 48 hours postinfusion, blood was collected via tail vein bleed and assayed for proinflammatory cytokines (IFN- γ , TNF- α , IL-12, and IL-6). Graph shown is a plot of the average of serum cytokine value with standard deviations.

much higher doses. The 0.128 and 0.384 mg/kg dosed mini-pigs reported here received an equivalent of 25 and 75 μ g dose per 20g mouse, an human equivalent dose of 0.0846 and 0.2538 mg/kg, respectively.

Most pigs on the treatment arm did experience temperature elevation on the first dosing day. Also, transient elevation of liver function tests was observed in the high-dose cohort but was not significant in the low dose cohort. Findings consistent with central line thrombus dispersion were observed in both control and treated pigs. Although not attributable to pbi-shRNA EWS/FLI1 LPX activity, the embolic pulmonary changes that resulted limited LPX-specific evaluation thus necessitating closer pulmonary monitoring in clinical testing. Notably, the low-dose cohort in this report (human equivalent dose of 0.08 mg/kg/70 kg) is higher than the 0.06 mg/kg dose of lipoplex established as the MTD by Roth *et al.*⁴⁹ with IV administration of TUSC2(FUS1)-LPX. Other DNA/liposome therapeutics are associated with a transient flulike syndrome and tachycardia in patients (*i.e.*, SGT-53 (ref. 72)). It is possible that with further dose escalation of the pbi-shRNA EWS/FLI1 LPX platform technology a similar toxicity profile may be observed however, based on the murine and pig experience with pbi-shRNA EWS/FLI1 LPX and human experience with both *FURIN* and *STMN1* bi-shRNA LPX products, there is a high likelihood that effective knockdown of *EWS/FLI1* will occur at dose levels below the toxicity limit thereby resulting in an acceptable therapeutic window.

In conclusion, *in vivo* efficacy with the pbi-shRNA EWS/FLI1 LPX was demonstrated in the Ewing's Sarcoma xenograft (SK-N-MC) characterized by the type-1 EWS/FLI1 fusion. Tolerance across dose levels was shown to be manageable. These data (in conjunction with previous clinical experience with other bi-shRNA LPX) are the basis for phase 1 testing of pbi-shRNA EWS/FLI1 LPX in poor prognosis patients with advanced Ewing's sarcoma with the type 1 fusion gene.

MATERIALS AND METHODS

Cell lines, DNA, liposome, and lipoplex. SK-N-MC (ATCC HTB-10 Ewing's sarcoma Type I fusion gene cell line) cells and HEK-293 (embryonic kidney cell line not containing EWS/FLI1 fusion) cells were purchased from ATCC (Manassas, VA). Research-grade plasmid DNA was purchased from Aldevron (Fargo, North Dakota). Waisman Biomanufacturing (Madison, WI) manufactured good manufacturing practice (GMP)-grade bi-shRNA EWS/FLI1 plasmid. GMP-grade liposome and pbi-shRNA EWS/FLI1 LPX was manufactured at Strike Bio (Carrollton, TX). Product release criteria and stability assessments were recently completed (Lot # 031815B-P).

In vitro growth inhibition. Cell proliferation assay was conducted by using the CellTiter-Glo Luminescent Cell Viability Assay Reagents by Promega (Madison, WI). Cells were transfected with differing amounts of plasmid DNA via optimized electroporation condition; parallel transfections were performed with reporter expressing plasmids to assess transfection efficiency. Transfected cells were seeded in 96-well opaque-walled culture plates at about 30% confluency. One to two days after transfection, the media were discarded, cells washed once with phosphate-buffered

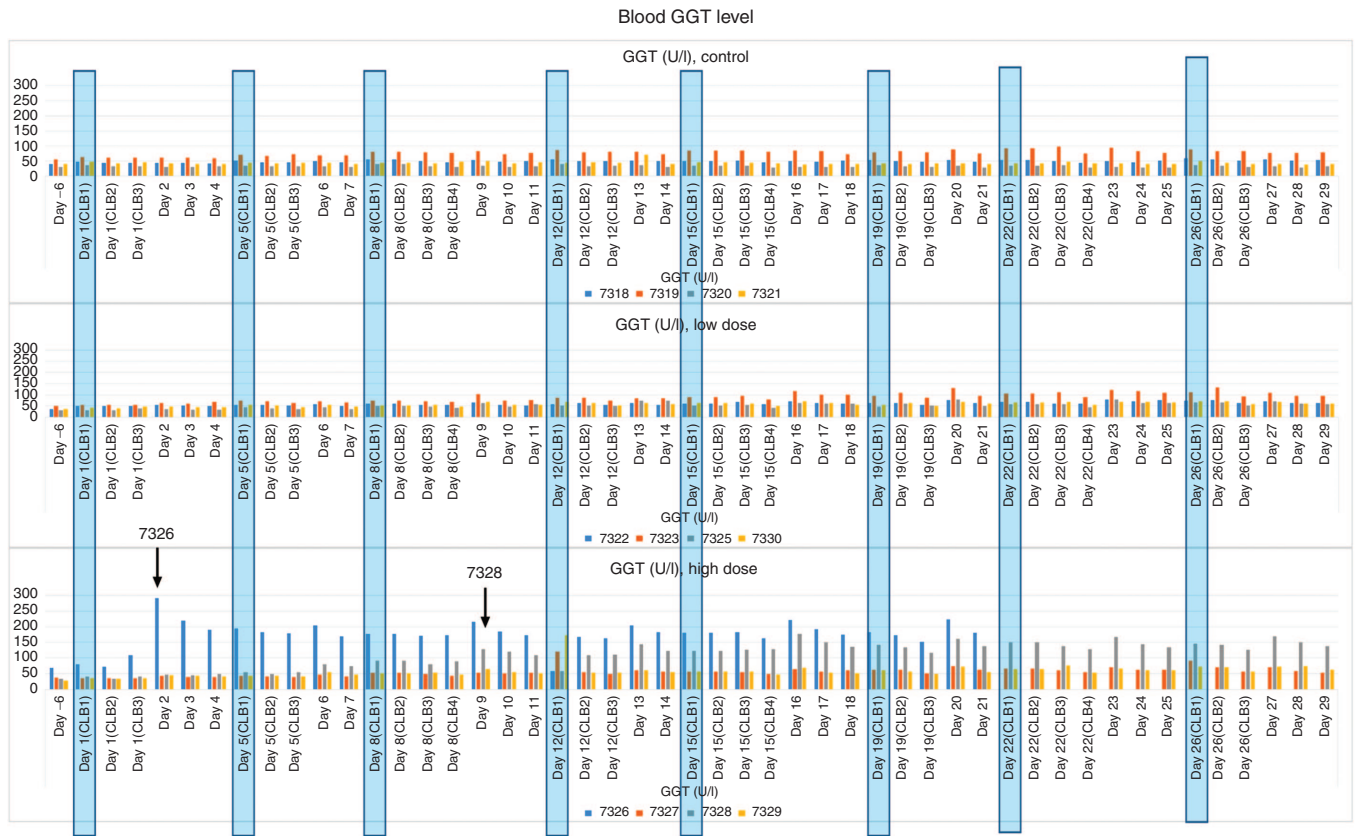


Figure 6 Blood GGT level. Comparison of GGT levels representative as assessment of liver function between control LPX ($n = 4$), pbi-shRNA^{EWS/FLI1} LPX 0.128 mg/kg dose group ($n = 4$) and pbi-shRNA^{EWS/FLI1} LPX 0.384 mg/kg dose group ($n = 4$) tracked throughout the entire dose schedule (eight doses administered/2x per week). Shaded box indicates treatment dates.

Table 1 Mini-pig premedication progression and equivalent patient premedication progression

Mini-pig		Human	
24 hours prior	Day 1	24 hours prior	Day 1
	Famotidine 10 mg IV (0.5 mg/kg) (30 minutes prior)	20 mg po qd X5d Aciphex or PPI	
Dexamethasone 6 mg IV (0.3 mg/kg)	Dexamethasone 6 mg IV (0.3 mg/kg) (1 hour prior)	8 mg oral dexamethasone	8 mg oral dexamethasone (1 hour prior)
	Diphenhydramine 12.5 mg IV (0.625 mg/kg) (30 minutes prior)		25 mg indocin (1 hour prior)
	Meloxicam 4 mg IV (0.2 mg/kg) (30 minutes prior)		650 mg acetaminophen (1 hour prior)

saline (PBS) then incubated with CellTiter-Glo reagent first on an orbital shaker for two minutes and then at room temperature for 10 minutes without shaking. The luminescent readings were obtained with a Luminometer plate reader (Thermo LabSystems) right after the incubation. All data points were in triplicate.

Protein expression by western immunoblot analysis. Tumor samples were first weighed and homogenized in CellLytic MT Cell Lysis Reagent for mammalian tissues (Sigma, St. Louis, MO) with 1x protease inhibitors (Sigma), 1x phosphatase inhibitors 2 (Sigma) and 1x phosphatase inhibitors 3 (Sigma) at ratio of 10 µl of lysis buffer to 1 mg tumor sample. The homogenates were centrifuged at 14,000 rpm for 10 minutes and the supernatants transferred to a clean tube. The protein concentration was measured using the Bradford method. An appropriated aliquot of tissue lysate from each sample was mixed with 1/3 volume of 4x Laemmli Sample buffer (Bio-Rad, Hercules, CA) with 5% β-mercaptoethanol and heated at 94 °C for 10 minutes. Then, samples were loaded on 4–20% Mini-PROTEAN TGX Precast Gels (Bio-Rad) for

electrophoresis. Afterwards, the protein in the gel was transferred to polyvinylidene difluoride membrane using Trans-Blot Turbo Transfer System (Bio-Rad). The membrane was first blocked with 5% non-fat milk in 1x PBS with 0.1% Tween 20 for 1 hour at room temperature, then probed with primary antibody in 5% non-fat milk in 1x PBS with 0.1% Tween 20 overnight at 4 °C. The next day, the membrane was washed three times with 1x PBS with 0.1% Tween 20 and then incubated for 2 hours with horseradish peroxidase-conjugated second goat anti-mouse (sc-2005) or goat anti-rabbit (sc-2004) antibody (Santa Cruz, Dallas, TX). After washing three times with 1x PBS with 0.1% tween 20, SuperSignal West Dura Extended Duration Substrate (ThermoFisher Scientific, Waltham, MA) was added to visualize the signal and the signal was captured using the ChemiDoc MP Imaging System (Bio-Rad). To detect EWS/FLI-1 fusion protein, 40 µg total protein lysate was loaded to run the gel and anti-FLI-1 antibody (AbCam, ab133485) was used. To detect CD99, 10 µg total protein lysate and anti-CD99 antibody (AbCam, ab108297) was used. Anti-β-actin antibody (C4) from Santa Cruz was used for normalization.

Lipoplex and physical characterization. The pbi-shRNA EWS/FLI1 LPX final product was manufactured under cGMP conditions (Strike Bio, Carrollton, TX). The manufacturing process follows a modified two-step ethanol injection method. Briefly, appropriate amounts of the lipids (DOTAP + Cholesterol) are weighed out and dissolved in ethanol. The liposomes (LP) are created by rapidly injecting a DOTAP:Cholesterol + Ethanol solution into 5% dextrose (D5W). The ethanol is removed by tangential flow filtration (TFF) with exchanges of D5W to reduce the ethanol concentration to less than 0.5%. The liposomes are then volume adjusted with additional D5W so that the final concentration is 10 mmol/l DOTAP and 9 mmol/l Cholesterol. Intermediate quality control is performed to confirm the physical characteristics of the liposomes before moving to the next series of manufacturing steps. The final product is created by rapidly mixing bi-shRNA EWS/FLI1 DNA with the liposomes to generate the pbi-shRNA EWS/FLI1 LPX product, at a concentration of 0.4 mg DNA/ml. The final product is vialled and held in quarantine until completion of all release testing.

Release testing includes LPX physical characterization (OD400, Z-average size, polydispersity index, and zeta potential), DNA identity and integrity analysis (DNA extraction and restriction enzyme digest), and purity assessment (thin layer chromatography, sterility, and endotoxin).

In vivo efficacy studies. Three *in vivo* mouse xenograft studies were designed to evaluate the efficacy of the pbi-shRNA EWS/FLI1 LPX product. All three murine studies were performed by an independent facility, Charles River Laboratories (Morrisville, NC). The first two studies (#e203, e204/e205) utilized our "prior thin film" manufacturing method.^{55,63,65,73,74} The third study (e207/e208) utilized the ethanol injection method described above.

The e203 study. In a pilot study, female athymic nude mice were implanted subcutaneously with SK-N-MC xenografts ($n = 10$ per group) and treatment began when the mean tumor volume was 120–180 mm³. Mice received a slow IV infusion of test article twice weekly for 4 weeks at a dose of 5 or 25 µg of pbi-shRNA EWS/FLI1 LPX per injection. Body weight and tumor volume were measured twice weekly and individual animals were taken off study when tumor volume reached 2,000 mm³. Statistical analysis was performed to detect significant differences between treatment groups and the controls.

The e204/e205 study. A follow-up study was performed using four additional doses to assess tumor growth delay (Study e204) and to sample tumor for molecular analysis (Study e205). For Study e204, female athymic nude mice ($n = 10$ per group) with SK-N-MC xenografts were treated with slow IV infusion twice weekly for 6 weeks. The treatment was started when tumor reached a range of 115–117 mm³. Four dose levels (25, 18.75, 12.5, and 6.25 µg per infusion) were tested. Study e204 was designed to follow body weight and tumor growth until the maximum allowable tumor volume was reached (similar to study e203 above). Study e205 (two animals per group) was designed to sacrifice all animals after 2 weeks of test article infusions and collect blood and tumor samples for molecular analysis.

The e207/e208 study. A third mouse xenograft study was designed, expanding upon the results of e203/e204/e205 studies. Female athymic nude mice were implanted with SK-N-MC xenografts ($n = 10$ per group) and treatment began when the tumor size was in the range 100 – 150 mm³. The e207/e208 study utilized the improved pbi-shRNA EWS/FLI1 LPX product (rapid injection method: vide infra) allowing for the exploration of higher doses (25 µg, 50 µg, and 75 µg) to test for efficacy and safety. The e207 Study followed a twice weekly × 4-week infusion schedule and measured body weight and tumor volume twice weekly until the individual maximum tumor volume was reached. The e208 study was designed to collect blood, kidney, lung, liver, and tumor for molecular analysis, two groups of three animals per group were either not treated or treated for 2 weeks with 75 µg of pbi-shRNA EWS/FLI1 LPX per infusion; animals were sacrificed 1 day after the last infusion.

In vivo pharmacology and toxicology study. Based on the results of the murine xenograft studies, a GLP swine pharmacokinetic/toxicology study was designed to prepare for IND submission. The pig study was performed by an independent facility, Charles River Laboratories (Spencerville, OH).

Yucatan mini pigs were chosen based on their bio-relevance to humans vis-s-vis possible off-target effects. Immature pigs were implanted with a telemetry device (for ECG, heart rate, and blood pressure monitoring) and a central venous access port (VAP) to be used for drug delivery and blood sample collection. Animals were dosed with pbi-shRNA EWS/FLI1 LPX (Lot # 031815B-P) ((0.128 mg/kg ($n = 2$ females + 2 males) or 0.384 mg/kg ($n = 2$ females + 2 males)) twice weekly × 4 weeks. Four (2 females + 2 males) control animals were treated with plasmid deficient liposome for comparison (vehicle control). The test article was diluted in 50 ml D5W and delivered over 30 minutes using an infusion pump. Premedication, equivalent to that used in patients (Table 1), was given to all 12 mini-pigs. Animals were monitored daily for well-being status and for clinical observations. Body temperature, heart rate, blood pressure, and electrocardiographic measurements were recorded at predefined time points following each test article infusion. In addition, blood samples were collected at defined time points following each infusion for hematology, coagulation, clinical chemistry, pharmacokinetic, and cytokine analysis. All animals were sacrificed 3 days after the final infusion. Full necropsy was performed and tissue samples were collected for histopathology and molecular analysis.

Cytokine analysis. Balb/C mice with average body weight of 20 g received single dose of 100 µg bi-shRNA EWS/FLI1 (Lot # 031815B-P) via slow tail vein infusion. At designated time points, postinfusion blood was collected via tail vein bleed into K2-EDTA tubes; plasma was prepared and stored at –80 °C before analysis. Cytokines (IFN-γ, TNF-α, IL-12, and IL-6) were assessed using a multiplex protein biomarker detection platform, Luminex MAGPIX system (Life Technologies, Carlsbad, CA). Twenty-five microliters of mouse plasma were first diluted four times in Bioplex Sample diluent. Fifty microliters of diluted plasma were added to 96-well plate containing beads with covalently coupled capture antibody to cytokines (each bead coupled with one type of capture antibody). At the same time, serial diluted mouse IFN-γ, TNF-α, IL-12, and IL-6 standards were also added to the plate in duplicate. After binding for 30 minutes in a shaker (at 850 rpm) at room temperature, beads were washed with buffer solution three times at room temperature to remove unbound proteins. Then biotinylated detection antibodies were added and incubated for 30 minutes. Unbound detection antibodies were removed by washing with wash solution three times at room temperature. Then SAPE solution was added to each well and signal was read using MAGPIX System. The raw data was further analyzed using Bioplex software and the absolute concentrations of the samples were determined by construction of a standard curve for each analyte.

ACKNOWLEDGMENTS

We gratefully acknowledge the generous support of the Alan B. Slifka Foundation, the Carson Sarcoma Foundation, the ChemoWarrior Foundation, Don and Linda Carter, the Helen L. Kay Charitable Trust, The Marilyn Augur Family Foundation, Michele Ashby, the Rutledge Foundation, the Speedway Children's Charities, Triumph Over Kid Cancer and the family and friends of Sam Day. The authors would like to acknowledge Michelle Watkins and Brenda Marr for their competent and knowledgeable assistance in the preparation of the manuscript. The following authors are shareholders in Gradalis, Inc. and Strike Bio: D.D.R., C.J., Z.W., J.N., and N.S. The authors have no other relevant affiliations or financial involvement with any organization or entity with a financial interest in or financial conflict with the subject matter or materials discussed in the manuscript.

REFERENCES

1. Leavey, PJ and Collier, AB (2008). Ewing sarcoma: prognostic criteria, outcomes and future treatment. *Expert Rev Anticancer Ther* **8**: 617–624.
2. Esiazhvili, N, Goodman, M and Marcus, RB Jr (2008). Changes in incidence and survival of Ewing sarcoma patients over the past 3 decades: Surveillance Epidemiology and End Results data. *J Pediatr Hematol Oncol* **30**: 425–430.
3. Gamberi, G, Cocchi, S, Benini, S, Magagnoli, G, Morandi, L, Kreshak, J *et al.* (2011). Molecular diagnosis in Ewing family tumors: the Rizzoli experience—222 consecutive cases in four years. *J Mol Diagn* **13**: 313–324.

4. Arvand, A and Denny, CT (2001). Biology of EWS/ETS fusions in Ewing's family tumors. *Oncogene* **20**: 5747–5754.
5. Tirode, F, Laud-Duval, K, Prieur, A, Delorme, B, Charbord, P and Delattre, O (2007). Mesenchymal stem cell features of Ewing tumors. *Cancer Cell* **11**: 421–429.
6. Riggi, N, Suvà, ML, Suvà, D, Cironi, L, Provero, P, Tercier, S et al. (2008). EWS-FLI-1 expression triggers a Ewing's sarcoma initiation program in primary human mesenchymal stem cells. *Cancer Res* **68**: 2176–2185.
7. Meltzer, PS (2007). Is Ewing's sarcoma a stem cell tumor? *Cell Stem Cell* **1**: 13–15.
8. Kovar, H, Ban, J and Pospisilova, S (2003). Potentials for RNAi in sarcoma research and therapy: Ewing's sarcoma as a model. *Semin Cancer Biol* **13**: 275–281.
9. Oikawa, T (2004). ETS transcription factors: possible targets for cancer therapy. *Cancer Sci* **95**: 626–633.
10. Toretzky, JA, Connell, Y, Neckers, L and Bhat, NK (1997). Inhibition of EWS-FLI-1 fusion protein with antisense oligodeoxynucleotides. *J Neurooncol* **31**: 9–16.
11. Tanaka, K, Iwakuma, T, Harimaya, K, Sato, H and Iwamoto, Y (1997). EWS-FlI1 antisense oligodeoxynucleotide inhibits proliferation of human Ewing's sarcoma and primitive neuroectodermal tumor cells. *J Clin Invest* **99**: 239–247.
12. Mateo-Lozano, S, Gokhale, PC, Soldatenkov, VA, Dritschilo, A, Tirado, OM and Notario, V (2006). Combined transcriptional and translational targeting of EWS/FLI-1 in Ewing's sarcoma. *Clin Cancer Res* **12**: 6781–6790.
13. Dohjima, T, Lee, NS, Li, H, Ohno, T and Rossi, JJ (2003). Small interfering RNAs expressed from a Pol III promoter suppress the EWS/FlI-1 transcript in an Ewing sarcoma cell line. *Mol Ther* **7**: 811–816.
14. Prieur, A, Tirode, F, Cohen, P and Delattre, O (2004). EWS/FLI-1 silencing and gene profiling of Ewing cells reveal downstream oncogenic pathways and a crucial role for repression of insulin-like growth factor binding protein 3. *Mol Cell Biol* **24**: 7275–7283.
15. Nozawa, S, Ohno, T, Banno, Y, Dohjima, T, Wakahara, K, Fan, DG et al. (2005). Inhibition of platelet-derived growth factor-induced cell growth signaling by a short interfering RNA for EWS-FLI1 via down-regulation of phospholipase D2 in Ewing sarcoma cells. *J Biol Chem* **280**: 27544–27551.
16. Kinsey, M, Smith, R and Lessnick, SL (2006). NR0B1 is required for the oncogenic phenotype mediated by EWS/FLI in Ewing's sarcoma. *Mol Cancer Res* **4**: 851–859.
17. Herrero-Martín, D, Osuna, D, Ordóñez, JL, Sevillano, V, Martins, AS, Mackintosh, C et al. (2009). Stable interference of EWS-FLI1 in an Ewing sarcoma cell line impairs IGF-1/IGF-1R signalling and reveals TOPK as a new target. *Br J Cancer* **101**: 80–90.
18. Hu-Lieskovan, S, Heidel, JD, Bartlett, DW, Davis, ME and Triche, TJ (2005). Sequence-specific knockdown of EWS-FLI1 by targeted, nonviral delivery of small interfering RNA inhibits tumor growth in a murine model of metastatic Ewing's sarcoma. *Cancer Res* **65**: 8984–8992.
19. Toub, N, Bertrand, JR, Tamaddon, A, Elhames, H, Hillaireau, H, Maksimenko, A et al. (2006). Efficacy of siRNA nanocapsules targeted against the EWS-FlI1 oncogene in Ewing sarcoma. *Pharm Res* **23**: 892–900.
20. Ramon, AL, Bertrand, JR, de Martimprey, H, Bernard, G, Ponchel, G, Malvy, C et al. (2013). siRNA associated with immunonanoparticles directed against cd99 antigen improves gene expression inhibition *in vivo* in Ewing's sarcoma. *J Mol Recog* **26**: 318–329.
21. Stahl, M, Ranft, A, Paulussen, M, Bölling, T, Vieth, V, Bielack, S et al. (2011). Risk of recurrence and survival after relapse in patients with Ewing sarcoma. *Pediatr Blood Cancer* **57**: 549–553.
22. Ozaki, T, Hillmann, A, Hoffmann, C, Rube, C, Blasius, S, Dunst, J et al. (1996). Significance of surgical margin on the prognosis of patients with Ewing's sarcoma. A report from the Cooperative Ewing's Sarcoma Study. *Cancer* **78**: 892–900.
23. Bacci, G, Picci, P, Ferrari, S, Mercuri, M, Brach del Prever, A, Rosito, P et al. (1998). Neoadjuvant chemotherapy for Ewing's sarcoma of bone: no benefit observed after adding ifosfamide and etoposide to vincristine, actinomycin, cyclophosphamide, and doxorubicin in the maintenance phase—results of two sequential studies. *Cancer* **82**: 1174–1183.
24. Klingebiel, T, Pertl, U, Hess, CF, Jürgens, H, Koscielniak, E, Pötter, R et al. (1998). Treatment of children with relapsed soft tissue sarcoma: report of the German CESS/CWS REZ 91 trial. *Med Pediatr Oncol* **30**: 269–275.
25. Rodriguez-Galindo, C, Billups, CA, Kun, LE, Rao, BN, Pratt, CB, Merchant, TE et al. (2002). Survival after recurrence of Ewing tumors: the St Jude Children's Research Hospital experience, 1979–1999. *Cancer* **94**: 561–569.
26. Shankar, AG, Ashley, S, Craft, AW and Pinkerton, CR (2003). Outcome after relapse in an unselected cohort of children and adolescents with Ewing sarcoma. *Med Pediatr Oncol* **40**: 141–147.
27. Barker, LM, Pendergrass, TW, Sanders, JE and Hawkins, DS (2005). Survival after recurrence of Ewing's sarcoma family of tumors. *J Clin Oncol* **23**: 4354–4362.
28. McTiernan, AM, Cassoni, AM, Driver, D, Michelagnoli, MP, Kilby, AM and Whelan, JS (2006). Improving Outcomes After Relapse in Ewing's Sarcoma: Analysis of 114 Patients From a Single Institution. *Sarcoma* **2006**: 83548.
29. Bacci, G, Ferrari, S, Longhi, A, Donati, D, De Paolis, M, Forni, C et al. (2003). Therapy and survival after recurrence of Ewing's tumors: the Rizzoli experience in 195 patients treated with adjuvant and neoadjuvant chemotherapy from 1979 to 1997. *Ann Oncol* **14**: 1654–1659.
30. Rasper, M, Jabar, S, Ranft, A, Jürgens, H, Amler, S and Dirksen, U (2014). The value of high-dose chemotherapy in patients with first relapsed Ewing sarcoma. *Pediatr Blood Cancer* **61**: 1382–1386.
31. Navid, F, Billups, C, Liu, T, Krasin, MJ and Rodriguez-Galindo, C (2008). Second cancers in patients with the Ewing sarcoma family of tumours. *Eur J Cancer* **44**: 983–991.
32. Merchant, TE, Kushner, BH, Sheldon, JM, LaQuaglia, M and Healey, JH (1999). Effect of low-dose radiation therapy when combined with surgical resection for Ewing sarcoma. *Med Pediatr Oncol* **33**: 65–70.
33. Saylor, RL 3rd, Stine, KC, Sullivan, J, Kepner, JL, Wall, DA, Bernstein, ML et al.; Pediatric Oncology Group. (2001). Cyclophosphamide plus topotecan in children with recurrent or refractory solid tumors: a Pediatric Oncology Group phase II study. *J Clin Oncol* **19**: 3463–3469.
34. Wagner, LM, McAllister, N, Goldsby, RE, Rausen, AR, McNall-Knapp, RY, McCarville, MB et al. (2007). Temozolomide and intravenous irinotecan for treatment of advanced Ewing sarcoma. *Pediatr Blood Cancer* **48**: 132–139.
35. Wagner, LM, Crews, KR, Iacono, LC, Houghton, PJ, Fuller, CE, McCarville, MB et al. (2004). Phase I trial of temozolomide and protracted irinotecan in pediatric patients with refractory solid tumors. *Clin Cancer Res* **10**: 840–848.
36. Wagner, LM (2010). Oral irinotecan for treatment of pediatric solid tumors: ready for prime time? *Pediatr Blood Cancer* **54**: 661–662.
37. Wagner, LM, Perentesis, JP, Reid, JM, Ames, MM, Safgren, SL, Nelson, MD Jr et al. (2010). Phase I trial of two schedules of vincristine, oral irinotecan, and temozolomide (VOIT) for children with relapsed or refractory solid tumors: a Children's Oncology Group phase I consortium study. *Pediatr Blood Cancer* **54**: 538–545.
38. Wagner, L, Turpin, B, Nagarajan, R, Weiss, B, Cripe, T and Geller, J (2013). Pilot study of vincristine, oral irinotecan, and temozolomide (VOIT regimen) combined with bevacizumab in pediatric patients with recurrent solid tumors or brain tumors. *Pediatr Blood Cancer* **60**: 1447–1451.
39. Casey, DA, Wexler, LH, Merchant, MS, Chou, AJ, Merola, PR, Price, AP et al. (2009). Irinotecan and temozolomide for Ewing sarcoma: the Memorial Sloan-Kettering experience. *Pediatr Blood Cancer* **53**: 1029–1034.
40. Raciborska, A, Bilka, K, Drabko, K, Chaber, R, Pogorzala, M, Wyrobek, E et al. (2013). Vincristine, irinotecan, and temozolomide in patients with relapsed and refractory Ewing sarcoma. *Pediatr Blood Cancer* **60**: 1621–1625.
41. McGregor, LM, Stewart, CF, Crews, KR, Tagen, M, Wozniak, A, Wu, J et al. (2012). Dose escalation of intravenous irinotecan using oral cefpodoxime: a phase I study in pediatric patients with refractory solid tumors. *Pediatr Blood Cancer* **58**: 372–379.
42. Navid, F, Willert, JR, McCarville, MB, Furman, W, Watkins, A, Roberts, W et al. (2008). Combination of gemcitabine and docetaxel in the treatment of children and young adults with refractory bone sarcoma. *Cancer* **113**: 419–425.
43. Mora, J, Cruz, CO, Parareda, A and de Torres, C (2009). Treatment of relapsed/refractory pediatric sarcomas with gemcitabine and docetaxel. *J Pediatr Hematol Oncol* **31**: 723–729.
44. Rapkin, L, Qayed, M, Brill, P, Martin, M, Clark, D, George, BA et al. (2012). Gemcitabine and docetaxel (GEMDOX) for the treatment of relapsed and refractory pediatric sarcomas. *Pediatr Blood Cancer* **59**: 854–858.
45. Rao, DD, Maples, PB, Senzer, N, Kumar, P, Wang, Z, Pappen, BO et al. (2010). Enhanced target gene knockdown by a bifunctional shRNA: a novel approach of RNA interference. *Cancer Gene Ther* **17**: 780–791.
46. Pizzorno, MC, O'Hare, P, Sha, L, LaFemina, RL and Hayward, GS (1988). trans-activation and autoregulation of gene expression by the immediate-early region 2 gene products of human cytomegalovirus. *J Virol* **62**: 1167–1179.
47. Zeng, Y, Cai, X and Cullen, BR (2005). Use of RNA polymerase II to transcribe artificial microRNAs. *Methods Enzymol* **392**: 371–380.
48. Matranga, C, Tomari, Y, Shin, C, Bartel, DP and Zamore, PD (2005). Passenger-strand cleavage facilitates assembly of siRNA into Ago2-containing RNAi enzyme complexes. *Cell* **123**: 607–620.
49. Lu, C, Stewart, DJ, Lee, JJ, Ji, L, Ramesh, R, Jayachandran, G et al. (2012). Phase I clinical trial of systemically administered TUSC2(FUS1)-nanoparticles mediating functional gene transfer in humans. *PLoS One* **7**: e34833.
50. Bernstein, M, Kovar, H, Paulussen, M, Randall, RL, Schuck, A, Teot, LA et al. (2006). Ewing's sarcoma family of tumors: current management. *Oncologist* **11**: 503–519.
51. Rocchi, A, Manara, MC, Scindria, M, Zambelli, D, Nardi, F, Nicoletti, G et al. (2010). CD99 inhibits neural differentiation of human Ewing sarcoma cells and thereby contributes to oncogenesis. *J Clin Invest* **120**: 668–680.
52. Zhang, PJ, Barcos, M, Stewart, CC, Block, AW, Sait, S and Brooks, JJ (2000). Immunoreactivity of MIC2 (CD99) in acute myelogenous leukemia and related diseases. *Mod Pathol* **13**: 452–458.
53. Waheed Roomi, M, Kalinovskiy, T, Roomi, NW, Niedzwiecki, A and Rath, M (2013). Inhibition of the SK-N-MC human neuroblastoma cell line *in vivo* and *in vitro* by a novel nutrient mixture. *Oncol Rep* **29**: 1714–1720.
54. Franzetti, GA, Laud-Duval, K, Bellanger, D, Stern, MH, Sastre-Garau, X and Delattre, O (2013). MiR-30a-5p connects EWS-FLI1 and CD99, two major therapeutic targets in Ewing tumor. *Oncogene* **32**: 3915–3921.
55. Barve, M, Wang, Z, Kumar, P, Jay, CM, Luo, X, Bedell, C et al. (2015). Phase I trial of Bi-shRNA STMN1 BIV in refractory cancer. *Mol Ther* **23**: 1123–1130.
56. Senzer, N, Barve, M, Kuhn, J, Melnyk, A, Beitsch, P, Lazar, M et al. (2012). Phase I trial of “bi-shRNA(furin)/GM-CSF DNA/autologous tumor cell” vaccine (FANG) in advanced cancer. *Mol Ther* **20**: 679–686.
57. Senzer, N, Nemunaitis, J, Barve, M, Orr, D, Kuhn, J, Magee, M et al. (2013) Long term follow up: phase I trial of “bi-shRNA furin/GM-CSF DNA/Autologous Tumor Cell” immunotherapy (FANG™) in advanced cancer *J Vaccines and Vaccination* **4**:209.
58. Rao, DD, Senzer, N, Cleary, MA and Nemunaitis, J (2009). Comparative assessment of siRNA and shRNA off target effects: what is slowing clinical development. *Cancer Gene Ther* **16**: 807–809.
59. Liu, SH, Rao, DD, Nemunaitis, J, Senzer, N, Zhou, G, Dawson, D et al. (2012). PDX-1 is a therapeutic target for pancreatic cancer, insulinoma and islet neoplasia using a novel RNA interference platform. *PLoS One* **7**: e40452.
60. Ghisoli, M, Barve, M, Schneider, R, Mennel, R, Lenarsky, C, Wallraven, G et al. (2015). Pilot Trial of FANG Immunotherapy in Ewing's Sarcoma. *Mol Ther* **23**: 1103–1109.
61. Nemunaitis, J, Barve, M, Orr, D, Kuhn, J, Magee, M, Lamont, J et al. (2014). Summary of bi-shRNA/GM-CSF augmented autologous tumor cell immunotherapy (FANG™) in advanced cancer of the liver. *Oncology* **87**: 21–29.
62. Phadke, AP, Jay, CM, Wang, Z, Chen, S, Liu, S, Haddock, C et al. (2011). *In vivo* safety and antitumor efficacy of bifunctional small hairpin RNAs specific for the human Stathmin 1 oncoprotein. *DNA Cell Biol* **30**: 715–726.
63. Templeton, NS, Lasic, DD, Frederik, PM, Strey, HH, Roberts, DD and Pavlakis, GN (1997). Improved DNA: liposome complexes for increased systemic delivery and gene expression. *Nat Biotechnol* **15**: 647–652.
64. Templeton, NS, Kumar, P, Sanchez, R, Templeton, N, Senzer, N, Maples, P et al. Non-viral vectors for the treatment of disease. in *Keystone Symposia on Molecular and Cellular Biology of Gene Therapy*. Salt Lake City, Utah, 1999.

65. Jay, CM, Ruoff, C, Kumar, P, Maass, H, Spanhel, B, Miller, M *et al.* (2013). Assessment of intravenous pbi-shRNA PDX1 nanoparticle (OFHIRNA-PDX1) in yucatan swine. *Cancer Gene Ther* **20**: 683–689.
66. Jay, C, Nemunaitis, G, Nemunaitis, J, Senzer, N, Hinderlich, S, Darvish, D *et al.* (2008). Preclinical assessment of wt GNE gene plasmid for management of hereditary inclusion body myopathy 2 (HIBM2). *Gene Regul Syst Bio* **2**: 243–252.
67. Wu, J, Liu, S, Yu, J, Zhou, G, Rao, D, Jay, CM *et al.* (2014). Vertically integrated translational studies of PDX1 as a therapeutic target for pancreatic cancer via a novel bifunctional RNAi platform. *Cancer Gene Ther* **21**: 48–53.
68. Liu, SH, Zhou, G, Yu, J, Wu, J, Nemunaitis, J, Senzer, N *et al.* (2013). Notch1 activation up-regulates pancreatic and duodenal homeobox-1. *Genes (Basel)* **4**: 358–374.
69. Ramesh, R, Saeki, T, Templeton, NS, Ji, L, Stephens, LC, Ito, I *et al.* (2001). Successful treatment of primary and disseminated human lung cancers by systemic delivery of tumor suppressor genes using an improved liposome vector. *Mol Ther* **3**: 337–350.
70. Judge, AD, Sood, V, Shaw, JR, Fang, D, McClintock, K and MacLachlan, I (2005). Sequence-dependent stimulation of the mammalian innate immune response by synthetic siRNA. *Nat Biotechnol* **23**: 457–462.
71. Robbins, M, Judge, A and MacLachlan, I (2009). siRNA and innate immunity. *Oligonucleotides* **19**: 89–102.
72. Senzer, N, Nemunaitis, J, Nemunaitis, D, Bedell, C, Edelman, G, Barve, M *et al.* (2013). Phase I study of a systemically delivered p53 nanoparticle in advanced solid tumors. *Mol Ther* **21**: 1096–1103.
73. Nemunaitis, G, Jay, CM, Maples, PB, Gahl, WA, Huizing, M, Yardeni, T *et al.* (2011). Hereditary inclusion body myopathy: single patient response to intravenous dosing of GNE gene lipoplex. *Hum Gene Ther* **22**: 1331–1341.
74. Nemunaitis, G, Maples, PB, Jay, C, Gahl, WA, Huizing, M, Poling, J *et al.* (2010). Hereditary inclusion body myopathy: single patient response to GNE gene Lipoplex therapy. *J Gene Med* **12**: 403–412.



This work is licensed under a Creative Commons Attribution-NonCommercial-NoDerivs 4.0 International License. The images or other third party material in this article are included in the article's Creative Commons license, unless indicated otherwise in the credit line; if the material is not included under the Creative Commons license, users will need to obtain permission from the license holder to reproduce the material. To view a copy of this license, visit <http://creativecommons.org/licenses/by-nc-nd/4.0/>

© DD. Rao *et al.* (2016)